



# Expression of asporin reprograms cancer cells to acquire resistance to oxidative stress

Yuto Sasaki<sup>1,2</sup> | Kurara Takagane<sup>1</sup> | Takumi Konno<sup>1,2</sup> | Go Itoh<sup>1</sup> | Sei Kuriyama<sup>1</sup> | Kazuyoshi Yanagihara<sup>3</sup> | Masakazu Yashiro<sup>4</sup>  | Satoru Yamada<sup>5,6</sup> | Shinya Murakami<sup>6</sup> | Masamitsu Tanaka<sup>1</sup> 

<sup>1</sup>Department of Molecular Medicine and Biochemistry, Akita University Graduate School of Medicine, Akita, Japan

<sup>2</sup>Department of Life Science, Faculty and Graduate School of Engineering and Resource Science, Akita University, Akita, Japan

<sup>3</sup>Division of Biomarker Discovery, Exploratory Oncology Research & Clinical Trial Center, National Cancer Center, Chiba, Japan

<sup>4</sup>Department of Surgical Oncology, Osaka City University Graduate School of Medicine, Osaka, Japan

<sup>5</sup>Department of Periodontology and Endodontology, Tohoku University Graduate School of Dentistry, Sendai, Japan

<sup>6</sup>Department of Periodontology, Osaka University Graduate School of Dentistry, Osaka, Japan

## Correspondence

Masamitsu Tanaka, Department of Molecular Medicine and Biochemistry, Akita University Graduate School of Medicine, Akita, Japan.  
Email: mastanak@med.akita-u.ac.jp

## Funding information

Takeda Science Foundation; Princess Takamatsu Cancer Research Fund, Grant/Award Number: 19-25123; Japan Society for the Promotion of Science, Grant/Award Number: 19H03495

## Abstract

Asporin (ASP), a small leucine-rich proteoglycan expressed predominantly by cancer associated fibroblasts (CAFs), plays a pivotal role in tumor progression. ASP is also expressed by some cancer cells, but its biological significance is unclear. Here, we investigated the effects of ASP expression in gastric cancer cells. Overexpression of ASP in 2 gastric cancer cell lines, HSC-43 and 44As3, led to increased migration and invasion capacity, accompanied by induction of CD44 expression and activation of Rac1 and MMP9. ASP expression increased resistance of HSC-43 cells to oxidative stress by reducing the amount of mitochondrial reactive oxygen species. ASP induced expression of the transcription factor HIF1 $\alpha$  and upregulated lactate dehydrogenase A (LDHA) and PDH-E1 $\alpha$ , suggesting that ASP reprograms HSC-43 cells to undergo anaerobic glycolysis and suppresses ROS generation in mitochondria, which has been observed in another cell line HSC-44PE. By contrast, 44As3 cells expressed high levels of HIF1 $\alpha$  in response to oxidant stress and escaped apoptosis regardless of ASP expression. Examination of xenografts in the gastric wall of ASPN<sup>-/-</sup> mice revealed that growth of HSC-43 tumors with increased micro blood vessel density was significantly accelerated by ASPN; however, ASPN increased the invasion depth of both HSC-43 and 44As3 tumors. These results suggest that ASPN has 2 distinct effects on cancer cells: HIF1 $\alpha$ -mediated resistance to oxidative stress via reprogramming of glucose metabolism, and activation of CD44-Rac1 and MMP9 to promote cell migration and invasion. Therefore, ASPN may be a new therapeutic target in tumor fibroblasts and cancer cells in some gastric carcinomas.

## KEYWORDS

asporin, gastric cancer, HIF1 $\alpha$ , oxidative stress, ROS

## 1 | INTRODUCTION

The cancer microenvironment affects cancer cell proliferation, invasion, and metastasis.<sup>1</sup> Most tumors are associated with a biologically

active type of fibroblast, known as reactive fibroblasts or cancer associated fibroblasts (CAFs). Although CAFs are variable, they usually have a profoundly negative impact on clinical outcome.<sup>2,3</sup> Previously, we have shown that asporin (ASP), also known as

This is an open access article under the terms of the Creative Commons Attribution-NonCommercial-NoDerivs License, which permits use and distribution in any medium, provided the original work is properly cited, the use is non-commercial and no modifications or adaptations are made.

© 2021 The Authors. Cancer Science published by John Wiley & Sons Australia, Ltd on behalf of Japanese Cancer Association.

periodontal ligament-associated protein 1 (PLAP1), is almost exclusively expressed by CAFs in gastric cancer specimens.<sup>4</sup>

ASPN is an extracellular matrix (ECM) protein that contains a unique D-repeat within its N-terminal region<sup>5</sup>; it belongs to the canonical class I family of small leucine-rich proteoglycans.<sup>6</sup> ASPN is found primarily in cartilage ECM surrounding skeletal tissue.<sup>7</sup> Expression of ASPN is elevated in degenerated intervertebral discs and it prevents periodontal ligament mineralization.<sup>8</sup> Polymorphisms in the D-repeat-sequence are associated with osteoarthritis.<sup>9</sup> In various tumors, ASPN is expressed mainly by stromal fibroblasts, which are positively associated with malignant potential in pancreatic, colorectal, gastric, and prostate cancers.<sup>10-15</sup> Polymorphisms in the D-repeat-sequence are also associated with prostate cancer progression.<sup>16</sup> In breast cancer, ASPN plays dual roles as it has both pro- and anti-tumor effects.<sup>17,18</sup> It also functions as a tumor suppressor gene in triple-negative breast cancer.<sup>19</sup>

Mechanistically, ASPN regulates the TGF- $\beta$ , EGFR, and CD44 signaling pathways.<sup>15</sup> ASPN binds to extracellular TGF- $\beta$ 1 or cytoplasmic Smad2/3 to inhibit or activate, respectively, the TGF- $\beta$  signaling pathway; this may explain why ASPN has pro-tumor<sup>11</sup> and anti-tumor<sup>19</sup> activities under different conditions. In addition, ASPN promotes activation of p-EGFR and its effector p-ERK1/2.<sup>13</sup> We also observed that ASPN secreted from CAFs activates Rac1 via interaction with CD44, thereby promoting invasion by CAFs.<sup>4</sup>

In addition to expression in fibroblasts, ASPN is expressed by some cancer cells. In colorectal cancer, ASPN promotes epithelial-mesenchymal transition (EMT), growth, migration, and metastasis by activating the TGF- $\beta$ /Smad2/3 or EGFR/Src/cortactin pathways.<sup>11,13,20</sup> In some gastric cancer cell lines, ASPN also accelerates cell proliferation via PSMD2 and by activating Erk, p38/MAPK, and PI3K/AKT signaling.<sup>21</sup> Because we also identified ASPN in cancer cells within some human gastric carcinoma specimens, we examined the function of ASPN in cancer cells. To better understand the biological significance of ASPN expression in cancer cells *in vivo*, it is necessary to exclude ASPN secreted from stromal fibroblasts. To this end, we implanted ASPN<sup>-/-</sup> mice with cancer cells expressing different amounts of ASPN.

In the present study, we demonstrate the importance of ASPN-mediated resistance of tumor cells to oxidative stress via upregulation of HIF1 $\alpha$ . ASPN expression increased the levels of HIF1 $\alpha$ , which shifted glucose metabolism to anaerobic glycolysis and reduced the amount of mitochondrial reactive oxygen species (mtROS), thereby attenuating ROS-induced apoptosis. ASPN in cancer cells also upregulated the expression of CD44, which further promoted cancer cell migration and invasion, leading to increased invasion depth of gastric cancer.

## 2 | MATERIALS AND METHODS

### 2.1 | Cell culture, transfection, and viral infection

CAFs from the tumoral gastric wall and normal fibroblasts (NFs) from the non-tumoral gastric wall were established as previously

described,<sup>22</sup> and cultured in DMEM containing 4500 mg/mL glucose, 1 mM sodium pyruvate, and 10% FBS. Gastric cancer cell line HSC-43, HSC-44PE, and 44As3 were established from patients with scirrhous gastric carcinoma.<sup>23,24</sup> 44As3 cells have strong potential for inducing the formation of peritoneal metastasis in the orthotopic mouse model.<sup>24</sup> Cells were transfected using Lipofectamine 2000 (Life Technologies). Recombinant lentiviral plasmids were co-transfected along with packaging vectors into 293T cells to allow the production of viral particles. HSC-43, HSC-44PE or 44As3 cells stably expressing asporin cDNA were established after viral infection by selection in medium containing puromycin. The selected cells were collected and used in bulk (HSC-43 ASPN, HSC-44PE ASPN), or cloned from single colonies (44As3 ASPN). In some experiments, ASPN was knocked down in HSC-43 ASPN cells using miRNAi (HSC-43 ASPN-miR) as described in Supplementary Material Appendix S1.

### 2.2 | Plasmids, antibodies, and reagents

Human cDNA encoding asporin (variant 1, corresponding to GenBank NM\_017680) was PCR-amplified from total cDNA synthesized from CAF-37, and the resulting cDNA was cloned into pCS2. To generate the recombinant lentivirus, cDNA was subcloned into the pCSII-CMV-MCS vector (RIKEN) with or without an HA-epitope tag at the carboxy terminus. Purchased antibodies were as follows: asporin (for immunoblot; Sigma-Aldrich HPA008435 St. Louis, MO USA, for immunohistochemistry; abcam Cambridge UK), MMP9 (Millipore Temeculo CA USA), Cytokeratin 19 (Agilent Santa Clara CA USA),  $\alpha$ SMA (Dako, Glostrup, Denmark), Vimentin (Cell Signaling Danvers, MA USA), CD44 (Cell Signaling), Rac1 (BD Biosciences Franklin Lakes, NJ USA), Cleaved caspase-3 (Cell Signaling), HIF1 $\alpha$  (for immunoblot; GeneTex, Irvine, CA USA, for immunohistochemistry; Sigma-Aldrich), Phospho-p38 MAPK (Cell Signaling),  $\alpha$ -tubulin (Santa Cruz, Dallas, Texas, USA), LDHA (Santa Cruz), Phospho-PDH-E1 $\alpha$  (Ser293) (Novus Bio), PDH-E1 $\alpha$  (Santa Cruz), Phospho-NF- $\kappa$ B p65 (Ser468) (Cell Signaling), Phospho-Akt (Ser473) (Cell Signaling), Akt (Cell Signaling), CD31 (Abcam). GST-asperin was purchased from Abnova (H00054829-P01). 3,3'-Diiodoacetylcarbocyanine perchlorate (DiO) and 1,1'-diiodoacetyl-3,3',3'-tetramethylindocarbocyanine perchlorate (DiI) were purchased from Thermo Fisher Scientific (Waltham, MA USA). Propylene glycol monomethylether acetate (PMA) was obtained from Sigma-Aldrich, and echinomycin was purchased from BioViotica (San Diego CA USA).

### 2.3 | Mice

PLAP-1 (asperin)<sup>-/-</sup> mice were generated using homologous recombination in embryonic stem cells in accordance with standard procedures at Osaka University (Yamada S, Murakami S).<sup>25</sup> KSN/Slc (*Foxn1<sup>nu</sup>*) mice were obtained from Japan Slc (Shizuoka, Japan). *PLAP-1<sup>-/-</sup>* mice were crossed with KSN/Slc mice to obtain

*PLAP-1<sup>-/-</sup>-Foxn1<sup>nu/nu</sup>* (designated ASPN<sup>-/-nu</sup>) nude mice. The mice were bred under specific pathogen-free conditions at the Animal Research Laboratory Bioscience Education-Research Center of Akita University. All animal protocols were approved by the Committee for Ethics of Animal Experimentation, and the experiments were conducted in accordance with the Guidelines for Animal Experiments (a-1-3175).

## 2.4 | 3D gel invasion assay

The assay was performed as described previously.<sup>4</sup> Briefly, 200  $\mu$ L of serum-free gel containing 2.25 mg/mL type-I collagen and 2.5 mg/mL Matrigel (BD Bioscience) was laid onto the upper chambers of Transwells in 24-well plates. Cancer cells were labeled with DiI, and fibroblasts were labeled with DiO, in accordance with the manufacturer's instructions: (i) Fibroblasts ( $2 \times 10^5$ ) were embedded in 600  $\mu$ L of gel in the upper chambers of Transwells (0.4- $\mu$ m pore). After the gels solidified, cancer cells ( $1 \times 10^5$ ) were overlaid onto the gels. (ii) This assay was performed as reported with modifications.<sup>26</sup> Gel was prepared as above and poured into 24-well plates. Immediately after gel pouring, the plastic rod (3-mm diameter) was hung down and suspended in the gel. After the gel solidified, the rod was pulled out to leave a pit in the solidified gel. Cancer cells ( $2 \times 10^5$ ) and fibroblasts ( $6 \times 10^4$ ) were mixed and suspended in 10  $\mu$ L of the gel described above, and then poured into the pit. In both assays, fixed gels were observed under a confocal microscope (LSM780, Zeiss, Oberkochen, Germany). Z-stacks of the X-Y plane were 3D-reconstructed using Zen software (Zeiss). The area of invading cells was quantified using ImageJ software (NIH, Bethesda, Maryland, USA). The invasion area was calculated, and shown as the ratio of the objective cells to the control cells.

## 2.5 | Evaluation of mtROS

To evaluate mtROS, MitoSOX<sup>®</sup> Red (Thermo Scientific), a mitochondrial superoxide indicator, was added to living cells at 5  $\mu$ M in accordance with the manufacturer's instructions. In some experiments, labeled cells were detached by trypsin, and subjected to flow cytometry analysis on the BD FACSAria<sup>™</sup> III system (BD Biosciences). In some experiments, labeled cells were fixed, and subjected to immunofluorescence staining with anti-HIF1 $\alpha$  antibody (Sigma-Aldrich) and Alexa-Fluor-488 goat anti-rabbit IgG (Life Technologies, Rockville, MD, USA).

## 2.6 | In vivo invasion assay

All animal experimental protocols were approved by the Committee for Ethics of Animal Experimentation, and the experiments were conducted in accordance with the Guidelines for Animal Experiments at Akita University. Invasion into the gastric

wall of tumors was tested by submucosal injection of tumor cells ( $1 \times 10^6$  each), suspended in 30  $\mu$ L of medium, into 6-wk-old ASPN<sup>-/-</sup> KSN nude mice. We used 5 mice for each group, and repeated each experiment twice. The mice were sacrificed 22 d after injection. Dissected stomachs were fixed, embedded in paraffin and sectioned for hematoxylin and eosin (HE) staining and immunohistochemistry. Invasion depth was evaluated in the specimens of maximum cut surface of each tumor.

## 2.7 | Specimens from cancer patients

Gastric cancer specimens were obtained from 30 patients who had undergone resection of primary gastric tumors. None of the patients had undergone preoperative radiation or chemotherapy. All samples were collected from the surgical pathology files at Akita University Hospital, Akita, Japan, between 2008 and 2013 and tissues were obtained with the informed consent of the patients.

## 2.8 | Statistical analysis

Statistical significance was calculated using Student *t* test. *P*-values < .05 were considered significant.

# 3 | RESULTS

## 3.1 | Expression of ASPN in gastric cancer cells

ASPN expression in archived human gastric carcinoma specimens was first assessed by immunohistochemical analysis. In non-cancer regions, ASPN expression was not detected in either stromal cells or epithelial glandular cells (Figure 1A). ASPN was detected most frequently in vimentin-positive mesenchymal cells in tumor stroma (Figure 1C; 65%, *n* = 40). Within the mesenchymal cells, ASPN was at least partially overlapped with  $\alpha$ SMA-positive CAFs (Figure 1C). However, it was also detected in cancer cells from some patients (10%). Typically, granular staining of ASPN was observed within epithelial cells lining the cancer glands (Figure 1B,C,E). ASPN staining was not detected in early stage cases in which the cancer cells remained in the mucosal layer (Figure 1D). Specific staining of ASPN was validated by pre-absorption of the detection antibody with recombinant ASPN, which reduced the intensity of granular staining in cancer cells (Figure 1E).

## 3.2 | ASPN expression in cancer cells promotes migration and invasion

To evaluate the effects of ASPN expression in cancer cells, we over-expressed it in HSC-43 and 44As3 gastric scirrhous carcinoma cells (termed HSC-43 ASPN and 44As3 ASPN, respectively) in which no

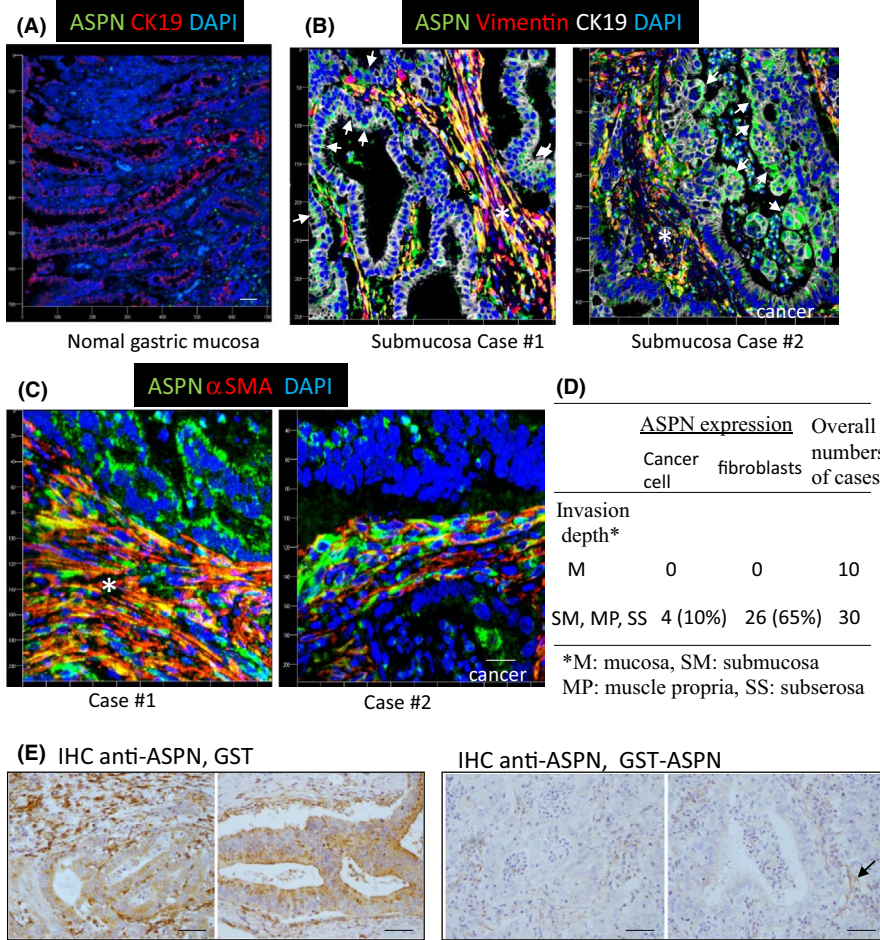


**FIGURE 1** Asporin is expressed by some gastric cancer cells. A–D, Human gastric cancer specimens (40 cases) were immunostained with an anti-ASPN antibody followed by 3,3'-diaminobenzidine. The results are summarized in (D). Samples in which cancer cells were positive for ASPN staining were selected and subjected to multicolored fluorescence immunostaining. Representative images are shown. Nuclei are stained with DAPI (blue). Bar, 50  $\mu$ m. A, Non-cancerous region of the gastric mucosa. B, C, Cancer regions in each case. Asterisks and arrows indicate ASPN staining in the stroma and in cancer cells, respectively. B, Co-immunostaining with antibodies against ASPN (green), vimentin (red) and cytokeratin-19 (CK19, white). C, ASPN (green) and  $\alpha$ SMA (red). E, Validation of the antibody. Immunohistochemical analysis of ASPN in case #1 using the primary antibody pretreated with control GST (left panels) or GST-ASPN (right panels). The arrow indicates a remaining weak signal in stromal fibroblasts. Bars, 50  $\mu$ m

endogenous ASPN was detected (Figure S1). When the motility of these cells was examined in a Transwell assay, overexpression of ASPN in both HSC-43 and 44As3 increased cell migration markedly (Figure 2A,B).

In tumor fibroblasts, ASPN stimulates cell migration by binding to CD44 and activating Rac1, which is a small GTPase that plays essential roles in cytoskeletal modification.<sup>4</sup> Expression of CD44 mRNA and protein was upregulated significantly by ASPN (Figure 2C). Activation of Rac1 was detected in both HSC-43 ASPN and 44As3 ASPN cells (Figure 2D). Therefore, ASPN activates the Rac1 pathway by controlling expression of CD44.

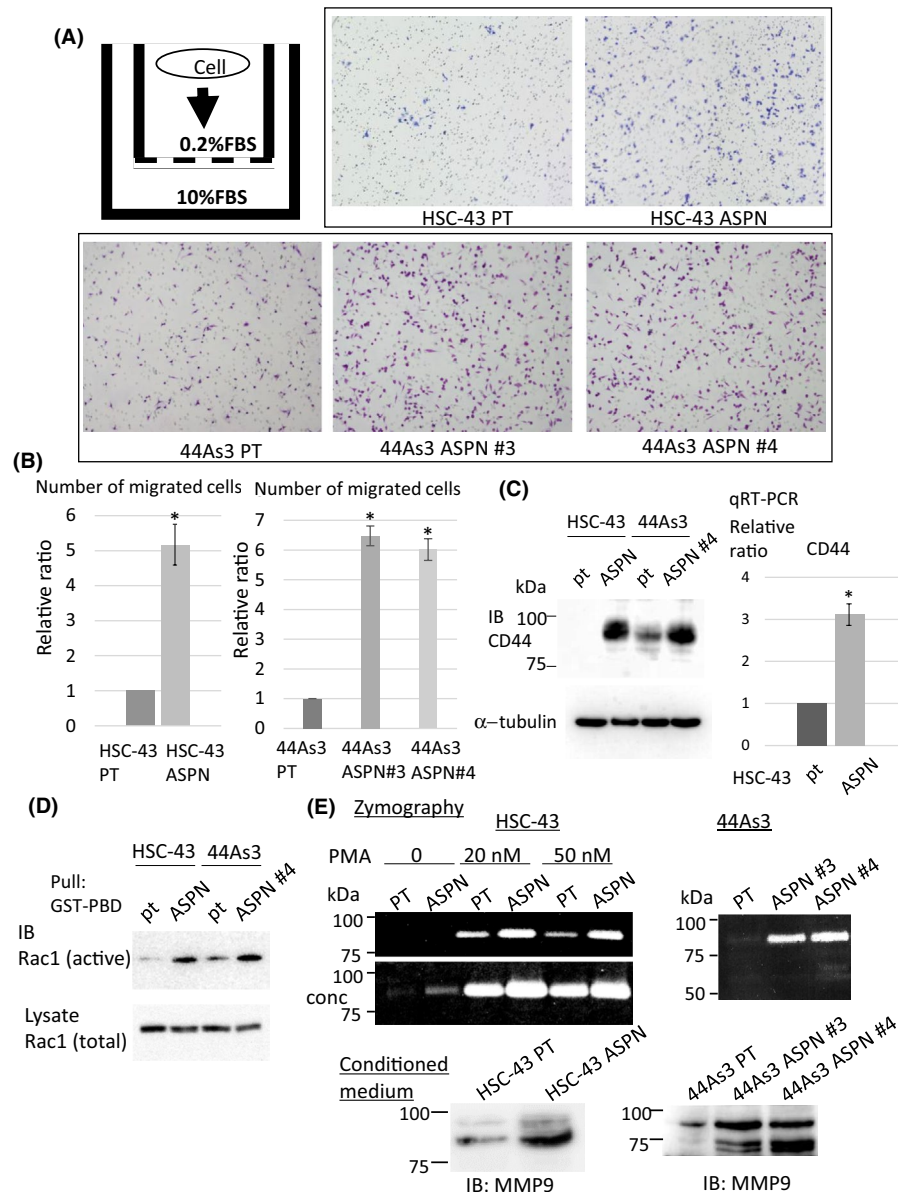
When conditioned medium (CM) from HSC-43 cells was examined in a gelatin zymography assay, ASPN expression increased the gelatinolytic band at 90 kDa, which was further enhanced by addition of PMA (TPA) (Figure 2E, top, left panels). TPA is known to increase MMP9 mRNA expression via PKC- $\alpha$ /MEK/Erk pathway.<sup>27</sup> Immunoblot analysis of CM revealed elevated secretion of MMP9 (Figure 2E, lower). Increased gelatin degradation by MMP9 was also detected in 44As3 ASPN cells (Figure 2E, right panels). These results indicated that expression of ASPN in gastric cancer cells activates Rac1 and secretion of MMPs.

Next, we examined invasion of ASPN-expressing cancer cells in 3D gel invasion assays. Because these cancer cells alone did

not invade the extracellular matrix (ECM)-containing gel, we used an invasion assay that resembles invasion of cancer cells into the fibrous gastric microenvironment. First, gastric NFs were embedded in an ECM-gel and cancer cells were plated on top (Figure 3A). The area of invading cancer cells in the gel was then quantified. When examining control parent cells, we found that a small number of HSC-43 cells or 44As3 cells invaded the gel containing NFs. By contrast, expression of ASPN increased invasion by both HSC-43 cells and 44As3 cells significantly (Figure 3B–D).

Next, we performed another gel invasion assay to examine co-invasion by cancer cells and fibroblasts. HSC-43 and 44As3 cells were mixed with NFs and implanted into a pit within an ECM-derived gel (Figure 3E). At first, a mixture of cancer cells and NFs contracted and aggregated in the pit before expanding and invading the area outside pit. In some cases, the periphery of the pit was lined by stacked fibroblasts (Figure 3F,G; left). Expression of ASPN in HSC-43 cells increased invasion by cancer cells (Figure 3G–I). Moreover, HSC-43 ASPN cells triggered invasion by fibroblasts to a much greater extent compared with HSC-43 parent cells (Figure 3G–I). Similar results were obtained using 44As3 ASPN cells (Figure S2). These results indicated that ASPN in cancer cells not only activates cancer cell invasion but also stimulates invasion by surrounding fibroblasts.

**FIGURE 2** ASPN induces expression of CD44 and activates Rac1 signaling. A, B, Cancer cells were seeded onto a Transwell membrane in serum-free medium. After 20 h, the wells were harvested and cells that migrated to the bottom surface of the membrane were counted. Representative fields from each experiment are shown (results represent 3 independent experiments, each in duplicate, and are expressed as the relative ratio to control cells). \* $P < .01$ . C, Expression of CD44 in cancer cells was examined by western blotting (left) or qRT-PCR (right). The results of qRT-PCR are expressed as the relative ratio of ASPN-expressing cells to control cells. \* $P < .01$ . D, Cell lysates were prepared from cancer cells cultured under standard conditions, pulled-down by GST-PBD, and then immunoblotted with anti-Rac1 to detect GTP-bound Rac1 (activated Rac1). Expression of total Rac1 in the input is shown in the lower panel. E, Gelatin zymography of HSC-43 parent (PT) and HSC-43 ASPN (left), or 44As3 parent and 44As3 ASPN (right), cell supernatants. HSC-43 cells were treated (or not) with PMA, as indicated. Conc: the supernatants were concentrated as described in Materials and Methods. Lower panels: MMP9 expression in each cell supernatant was examined by western blot analysis



### 3.3 | ASPN protects cancer cells from oxidative stress-induced apoptosis

Next, we examined ASPN-mediated cellular responses to PMA. PMA causes oxidative stress by producing high amounts of superoxide radicals.<sup>28</sup> Treatment with a high concentration of PMA triggered apoptosis in parent HSC-43 cells after 12 h, however HSC-43 ASPN cells did not show apoptotic changes (Figure 4A). Consistent with this, PMA-induced expression of cleaved caspase-3 in HSC-43 parent cells, but this was far less evident in HSC-43 ASPN cells (Figure 4B).

ASPN increased expression of HIF1 $\alpha$ ; this increase was more significant after PMA treatment (Figures 4B and S3A). Because HIF1 $\alpha$  reduces intracellular ROS levels by reprogramming glucose metabolism from oxidative phosphorylation to anaerobic glycolysis, we next examined markers of metabolic reprogramming.<sup>29-32</sup> HSC-43 ASPN cells showed increased expression of lactate dehydrogenase

A (LDHA), which produces lactic acid, and phosphorylated pyruvate dehydrogenase-E1 $\alpha$  (PDH-E1 $\alpha$ ), which restricts synthesis of acetyl-CoA (Figure 4B).<sup>30</sup> By contrast, ASPN expression reduced levels of phospho-p38, a marker of ROS and oxidative stress (Figure 4B).<sup>32</sup> Moreover, these change of gene expression and activation were reversed by knockdown of ASPN in HSC-43 ASPN cells (HSC-43 ASPN-miR: Figures S1 and S3B). These results suggested that ASPN induces HIF1 $\alpha$  expression and reduces ROS in HSC-43 cells by reprogramming glucose metabolism. We further confirmed this conclusion by preparation of another ASPN over-expressing cell line; HSC-44PE ASPN (Figure S1). Similar results were obtained by HSC-44PE ASPN as HSC-43 ASPN; ASPN induced anaerobic glycolysis and resistance to PMA-induced oxidative stress (Figure S3C).

In contrast with HSC-43 cells, 44As3 cells were more resistant to PMA treatment. Parent 44As3 cells and 44As3 ASPN cells showed no apparent apoptotic changes after PMA treatment, although cleaved caspase-3 levels were slightly elevated (Figure S4A,C).

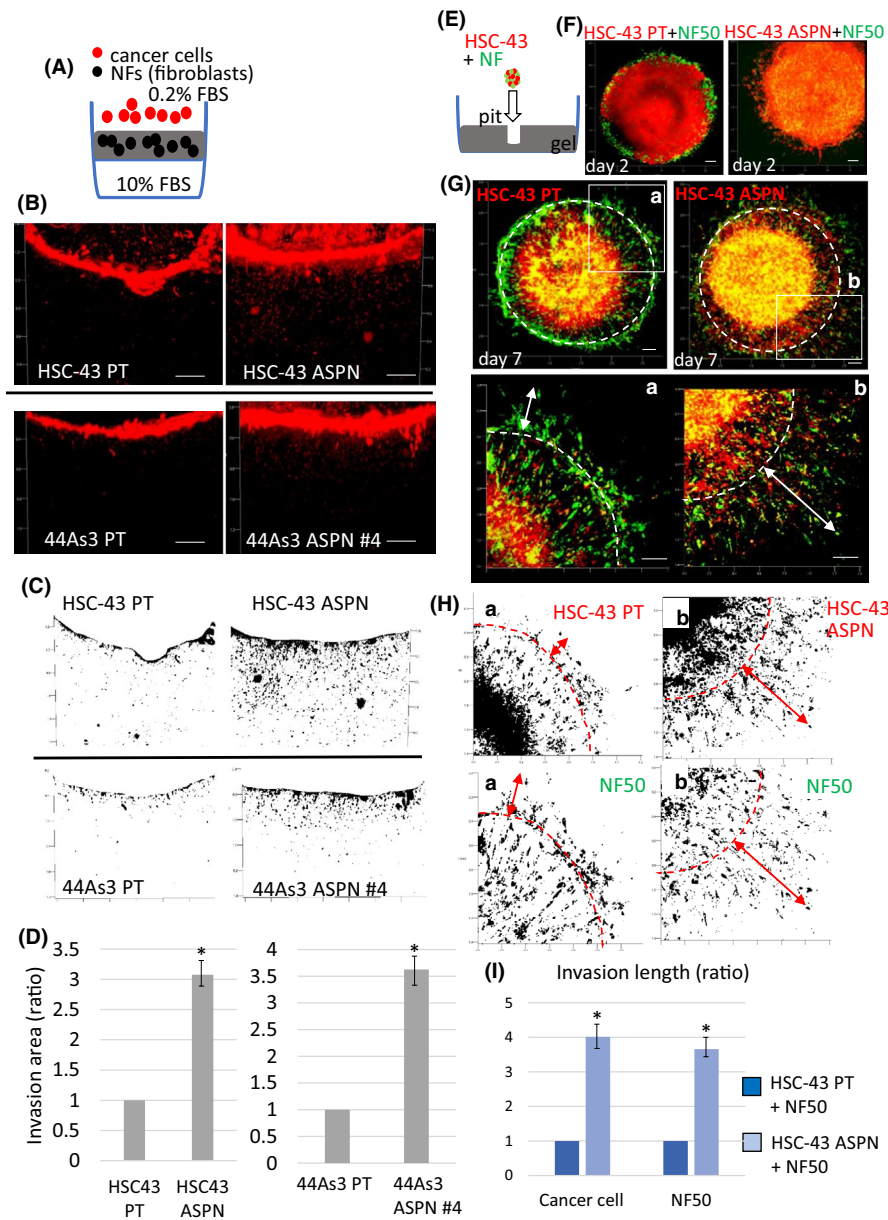


**FIGURE 3** ASPN promotes cancer cell invasion. A–D, Dil-labeled cancer cells were plated on a gel containing NFs. Images were taken after 7 d. Bars, 200  $\mu$ m. C, Quantitation of the cell invasion area. Invading cells are shown in black. D, The invasion area is expressed as the relative ratio to control parent cells. \* $P < .01$ . (E–I) Gels containing a 3 mm pit were generated in 24-well plates, and cancer cells (Dil labeled, red) and NFs (DiO labeled, green) were mixed and implanted into the pit. Images were taken after 2 d (F) or 7 d (G) of co-culture. Boxed areas in (G) are shown in the enlarged image at the bottom. Bars, 200  $\mu$ m. H, Quantitation of cell invasion distance. The dotted line indicates the pit periphery. Double-headed arrows indicate invasion distance, as determined by the cell that traveled the greatest distance from the pit periphery. I, Invasion distances of cancer cells or NF cells are shown as the relative ratio to control of HSC-43 parent cells and the NF mixture. \* $P < .01$

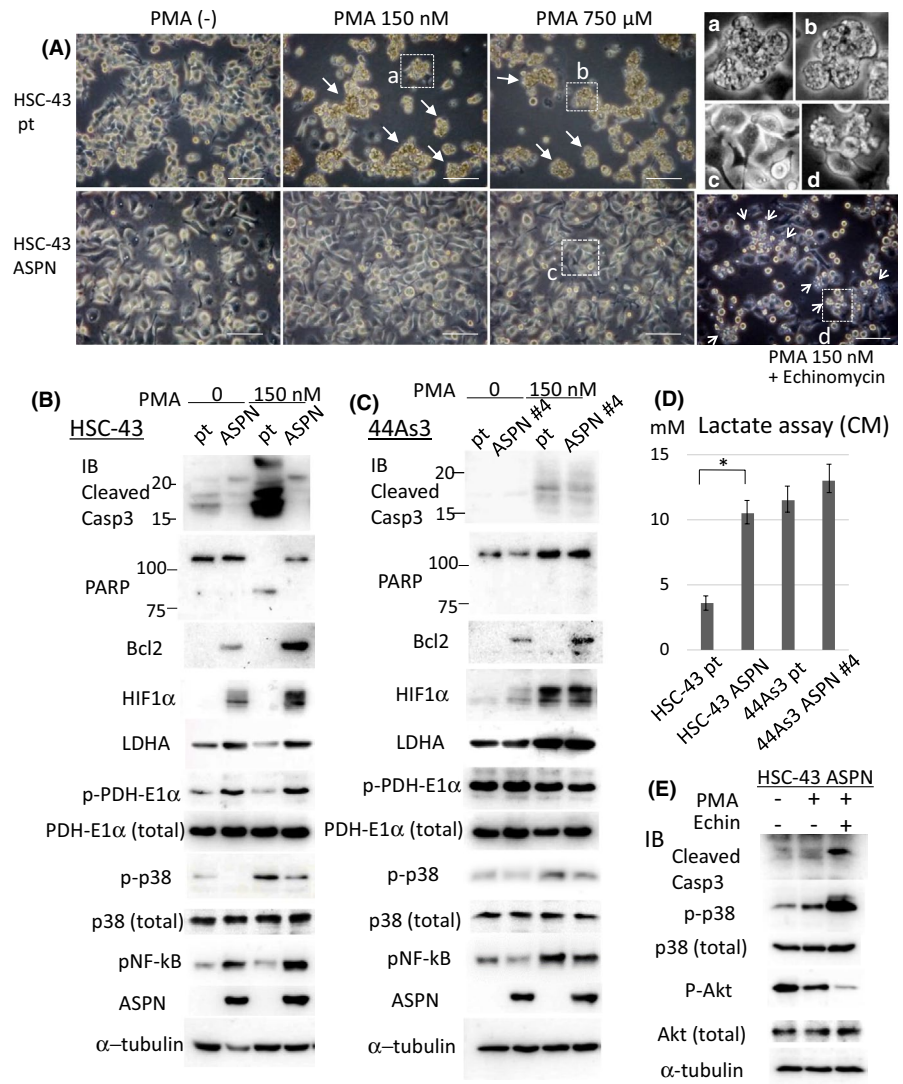
Marked expression of HIF1 $\alpha$  together with high amounts of LDHA and phosphorylated PDH-E1 $\alpha$ , and low levels of phospho-p38, were observed in both parent 44As3 cells and 44As3 ASPN cells after PMA treatment (Figure 4C). In addition, LDHA and phosphorylated PDH-E1 $\alpha$  was also detected at high level in untreated parent 44As3 cells, suggested that basal glucose metabolism of 44As3 cells rather shifts to anaerobic glycolysis (Figure 4C). Consistent with this finding, the amount of lactate in the CM of parent 44As3 cells was at a high level, although it was low in parent HSC-43 cells and significantly increased in HSC-43 ASPN cells (Figure 4D).

Hypoxia-mediated induction of HIF1 $\alpha$  in these cancer cell lines was examined. When cells were incubated under 1.0% oxygen, HIF1 $\alpha$  was significantly upregulated by ASPN, especially in HSC-43 cells, accompanied by elevation of LDHA and phosphorylated PDH-E1 $\alpha$  (Figure S4B). Conversely, in 44As3 cells, levels of LDHA and phosphorylated PDH-E1 $\alpha$  did not change by expression of ASPN

(Figure S4B). When the DNA-binding ability of HIF1 $\alpha$  was blocked by echinomycin, apoptosis of HSC-43 ASPN cells increased, accompanied by increased expression of cleaved caspase-3 (Figure 4A, lower right, and Figure 4E). Consistent with this finding, echinomycin decreased expression of phosphorylated Akt (which indicated reduced expression of activated Akt) and increased phospho-p38 in PMA-treated HSC-43 ASPN cells (Figure 4E).

We further examined superoxide levels in response to PMA treatment by labeling the cells with MitoSox, which detects mitochondrial superoxide by generating red fluorescence after oxidation of the probe. When PMA was added, red fluorescence increased to a greater extent in parent HSC-43 cells than in HSC-43 ASPN cells, indicating that ASPN expression reduced the amount of mitochondrial ROS (mtROS) (Figure 5A, left upper panels); this was confirmed by fluorescence activated cell sorting (FACS; Figure 5C, left). In addition, HIF1 $\alpha$  expression was more intense in the nucleus

**FIGURE 4** Aspirin protects cancer cells from oxidative stress. **A**, Appearance of HSC-43 and HSC-43 ASPN cells exposed to PMA (indicated above the panels). (Right lower) HSC-43 ASPN cells were treated with PMA together with echinomycin (0.1  $\mu$ M). Images were taken 12 h after addition of PMA to the medium. Arrows indicate aggregated apoptotic cells. Bars, 50  $\mu$ m. **B**, **C**, Cancer cells were treated with PMA or left untreated and then incubated for 12 h. Cell lysates were subjected to immunoblotting. **D**, Conditioned medium was collected from each cancer cells after incubation for 24 h under standard culture condition. Lactate in the medium was quantified as described in Materials and Methods. \* $P < .01$ . **E**, HSC-43 ASPN cells were treated with PMA (150 nM) with or without echinomycin (0.1  $\mu$ M) for 10 h. Cell lysates were prepared and subjected to immunoblotting with the indicated antibodies



of ASPN-expressing HSC-43 cells (Figure 5A, lower panels). By contrast, 44As3 cells showed rather high expression of HIF1 $\alpha$  and low expression of mtROS in both parent and ASPN cells (Figure 5A, right panels). Similar results were obtained under hypoxic conditions (Figure 5B,C).

### 3.4 | Aspirin promotes tumor growth

Next, we examined the *in vivo* effects of ASPN in cancer cells by implanting gastric cancer cells into the stomach of nude mice. To exclude the effects of ASPN expression in the tumor microenvironment, we used ASPN (PLAP-1)<sup>-/-</sup> nude mice; this was because native mice generate CAFs, which secrete high amounts of ASPN. When HSC-43 parent cells or HSC-43 ASPN cells were inoculated into the submucosal space (SM) of ASPN<sup>-/-nu</sup> mice, HSC-43 ASPN tumors were much larger than the control tumors (Figure 6A,B, left). In mice injected with 44As3 cells, tumor size was increased slightly by ASPN (Figure 6A,B, right). Histologically, HSC-43 ASPN cells invaded deep into the gastric wall, frequently penetrating the muscularis propria

(MP) and reaching the subserosal space in more than half of the mice, whereas control HSC-43 parent cells remained in the SM space in most cases (Figure 6C,D, left). Increased invasion depth was also observed in 44As3 ASPN tumors (Figures S5A, and 6D, right). The invasion depth data from injected mice are summarized in Figure 6E. Expression of ASPN and HIF1 $\alpha$  in HSC-43 cell tumors was confirmed by immunohistochemistry (Figure 6F,G). HIF1 $\alpha$  accumulated in the nucleus of HSC43 ASPN cells (Figure 6G), whereas it was detected in both 44As3 parent and 44As3 ASPN tumor cells (Figure S5B).

Because expression of ASPN in cancer cells affects tumor size, we examined micro blood vessel density using immunohistochemical analysis of CD31, a marker of endothelial cells, in the maximum cut surface of each tumor. The average number of CD31<sup>+</sup> blood vessels per tumor area was more than 2-fold higher in HSC-43 ASPN tumors than in the controls (Figure S6A–C), however it was not significantly different between 44As3 ASPN or 44As3 parent cells (data not shown).

To identify the mechanism underlying the increase in blood vessels in HSC-43 ASPN tumors, we used quantitative RT-PCR to examine expression of pro-angiogenic cytokines by cultured cells. We found that expression of mRNA encoding *Ang1* was

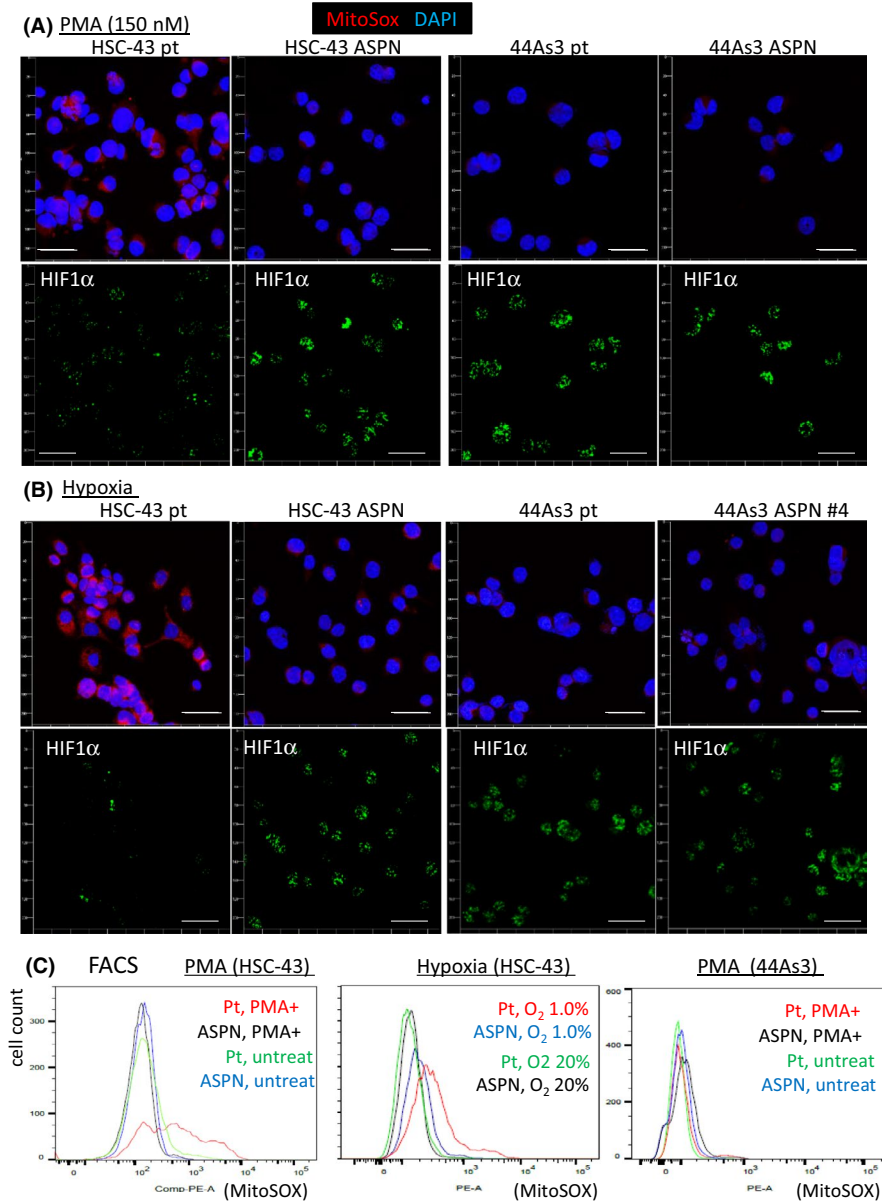


**FIGURE 5** Intracellular asporin reduces ROS levels in HSC-43 cells. A, B, Cancer cells were treated with PMA for 8 h (A) or subjected to hypoxic conditions (1.0% O<sub>2</sub>) for 48 h. B, Cells were labeled with MitoSOX Red, fixed, and immunostained with an anti-HIF1α antibody (bottom panels). Bars, 40 μm. C, Cancer cells were treated with PMA or subjected to hypoxia, labeled with MitoSOX Red, and subjected to FACS

significantly higher in HSC-43 ASPN cells compared with in control cells (Figure S6D).

## 4 | DISCUSSION

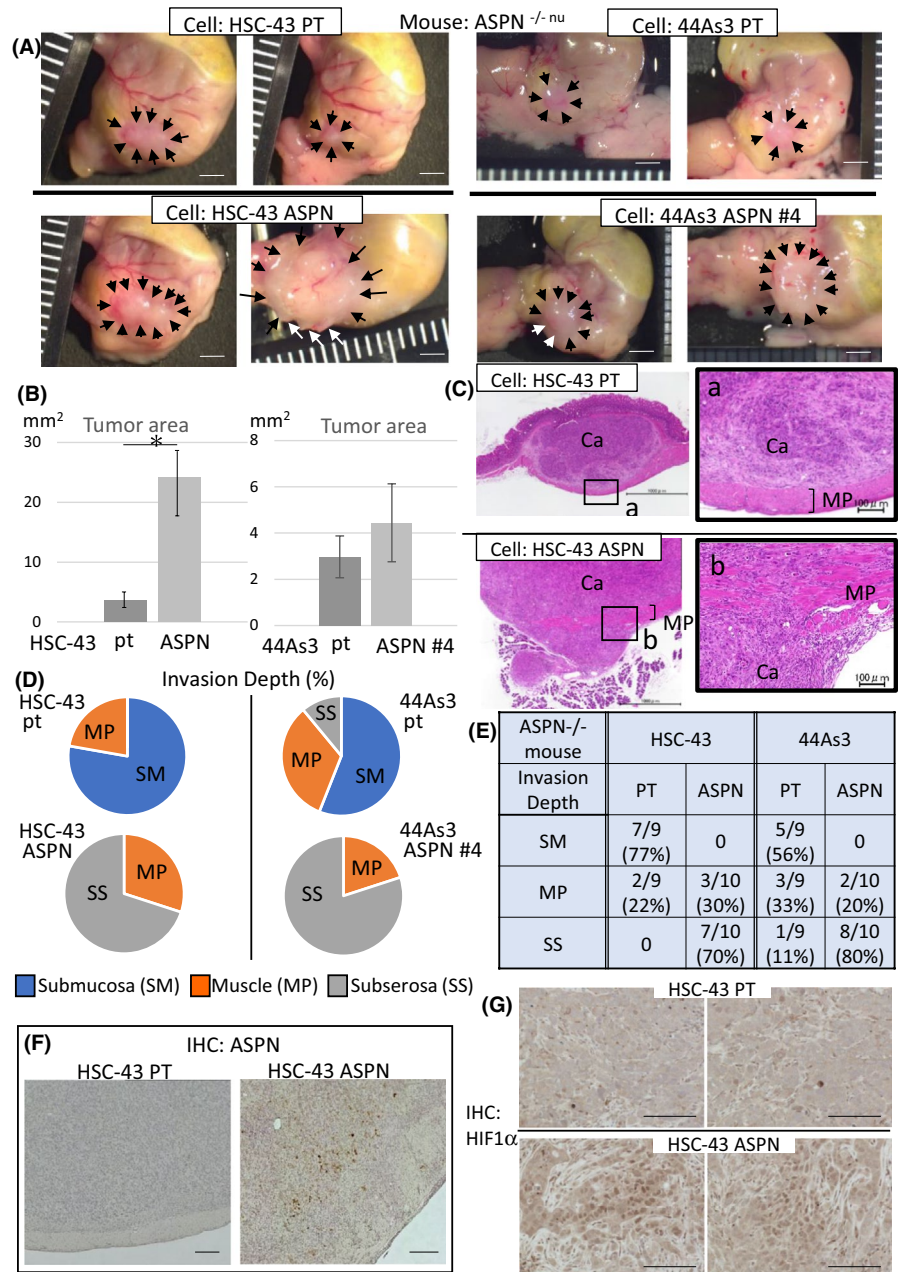
In gastric cancer, ASPN is largely expressed by CAFs. However, we also detected expression in gastric cancer cells in around 10% of archived tissues. Here, we examined the effects of ASPN in cancer cells. ASPN enabled gastric cancer cells to escape from PMA-induced oxidative stress by upregulating HIF1α. HIF1α induces LDHA and pyruvate dehydrogenase kinase 1 (PDK1), which phosphorylates PDH-E1α.<sup>33</sup> Elevation of LDHA and phosphorylation of PDH-E1α in HSC-43 ASPN cells and HSC-44PE ASPN cells suggest a shift to anaerobic glucose metabolism. LDHA produces lactate and proceeds lactic acid fermentation. Phosphorylated PDH-E1α is inactive and attenuates the ability of a cell to convert pyruvate to

acetyl-CoA, therefore it inhibits the Krebs cycle and drives the shift to an anaerobic pathway. Reprogramming cancer cells from oxidative phosphorylation to anaerobic glycolysis reduced the activity of mitochondria and reduces levels of mtROS (Figure S7A). In HSC-43 ASPN cells, we detected a significant reduction in mtROS after PMA treatment and/or hypoxic culture.

In addition, expression of ASPN by cancer cells upregulated CD44, which further promoted cancer cell migration and invasion. Extracellular secreted ASPN binds to cell membrane protein CD44 to activate Rac1. Therefore, because ASPN increases expression of CD44, the CD44-Rac1 axis drives migration and invasion. HIF1α protein levels are controlled mainly by post-translational modifications and protein degradation, however ASPN-mediated expression of HIF1α can be regulated at the mRNA level (Figure S2A), although the underlying mechanism is not clear. In addition, ASPN regulates NF-κB activity through HIF1α because both HIF1α and NF-κB p65 activate transcription.<sup>34</sup>



**FIGURE 6** Expression of asporin in cancer cells increases tumor size and invasion depth. Cancer cells were injected into the submucosal space of ASPN<sup>-/-nu</sup> nude mice. A, Appearance of the stomach 22 d after implantation of cancer cells. Arrows indicate the tumor periphery. Bars, 2 mm. B, Tumor area was determined using ImageJ software. \**P* < .01. C, Tumors were excised, fixed, and the maximum cut surface was subjected to H&E staining. Representative images are shown. Boxed areas are enlarged in the right panels. MP: muscle propria layer. Bars, 1 mm (left) and 100 μm (right panels). D, E, Invasion depth indicates the position of the cell that traveled furthest into the stomach wall, as determined by H&E staining, and expressed by which layer it existed. Percentage of total 9 or 10 mice of each group was shown. F, G, Immunohistochemical examination of ASPN and HIF1α expression in the xenografts. Bars, 100 μm



Extracellular ASPN secreted from mesenchymal stromal cells (MSC) binds to BMP-4 and inhibits BMP-4-induced MSC differentiation, which in turn regulates MSC self-renewal and multipotency.<sup>35</sup> Although expression of CD44, a marker of cancer stem cells (CSCs), was induced by ASPN, mRNA encoding other CSC markers (including CD133, SOX2, OCT4, and Nanog) was not upregulated in HSC-43 ASPN cells compared with parent cells (data not shown). Therefore, upregulation of CD44 does not suggest that ASPN increases the number of CSCs, rather it activates cell migration. CD44<sup>+</sup> cancer cells promote angiogenesis in some tumors, therefore the ASPN-CD44 interaction may also have angiogenic potential.<sup>36</sup>

ASPN is induced in the stromal mice fibroblasts of xenograft tumors. Therefore, to compare ASPN(+) or ASPN(-) cancer cells in vivo, we excluded stromal ASPN by using ASPN<sup>-/-</sup> mice. The effects of ASPN on tumor size and invasion by HSC-43 and 44As3

tumors were different. ASPN expression increased HSC-43 tumor size significantly, accompanied by increased blood vessel density; this was much less evident in 44As3 tumors. By contrast, ASPN promoted deeper invasion by both HSC-43 and 44As3 tumors. These results were largely consistent with the in vitro observations, ie, that HSC-43 and 44As3 cells showed different responses to PMA and hypoxia. HIF1α expression in HSC-43 cells was induced by ASPN, which significantly reduced the amount of intracellular ROS induced by PMA and hypoxia. However, 44As3 parent cells expressed high levels of HIF1α in response to PMA or hypoxia without expressing ASPN. In addition, 44As3 cell metabolism seemed to be anaerobic because PDH-E1α was highly phosphorylated (Figure 4C). Cancer cells with high malignant potential, like 44As3, often express HIF1α at high levels.<sup>37</sup> Indeed, invasion and peritoneal dissemination of 44As3 cells was greater than that of

HSC-43 cells or HSC-44PE (Figure 6D), thus the former may harbor other mechanisms that increase HIF1 $\alpha$  and PDK1 activation.<sup>24</sup> Because hypoxic conditions and oxidative stress are common in tumors, resistance to these phenomena is associated with tumor growth. By contrast, ASPN upregulated CD44 and activated Rac1 in both HSC-43 and 44As3 cells, suggesting that ASPN may play an essential role in cancer cell invasion in vivo.

Tumor cells are exposed to oxidative stress in various situations. ROS are generated by exposure of cancer cells to hypoxia, reperfusion, radiotherapy, and some chemotherapeutic agents.<sup>38</sup> Expression of ASPN in cancer cells may be important for resistance to these therapies and may play pivotal roles in post-therapy tumor relapse. Although the mechanism of upregulation of ASPN in cancer cells is not clear, activation of NF- $\kappa$ B, eg by IL-1 $\beta$  increases transcription of ASPN.<sup>39</sup> We also observed that lipopolysaccharide (LPS) induced ASPN expression in HSC-43 cells (Figure S7B). Therefore, one possibility is that severity of inflammation in tumors may modify ASPN levels in cancer cells. Further large-scale studies should examine the correlation between ASPN, tumor progression, and survival by evaluating ASPN expression in cancer cells and stromal cells separately.

#### ACKNOWLEDGMENTS

We thank members of the Bioscience Education and Research Support Center (BERSC) at Akita University for technical assistance. This work was supported by JSPS KAKENHI grants (19H03495 to M. Tanaka), a Research Grant from the Princess Takamatsu Cancer Research Fund (19-25123 to M. Tanaka), and the Takeda Science Foundation (to M. Tanaka).

#### CONFLICT OF INTEREST

The authors declare no competing financial interests. The authors disclose no potential conflicts of interest.

#### ORCID

Masakazu Yashiro  <https://orcid.org/0000-0001-5743-7228>

Masamitsu Tanaka  <https://orcid.org/0000-0002-4823-9737>

#### REFERENCES

- Yashiro M, Hirakawa K. Cancer-stromal interactions in scirrhous gastric carcinoma. *Cancer Microenviron*. 2010;3:127-135.
- Ungefroren H, Sebens S, Seidl D, Lehnert H, Hass R. Interaction of tumor cells with the microenvironment. *Cell Commun Signal*. 2011;9(1):18.
- Karagiannis GS, Poutahidis T, Erdman SE, Kirsch R, Riddell RH, Diamandis EP. Cancer-associated fibroblasts drive the progression of metastasis through both paracrine and mechanical pressure on cancer tissue. *Mol Cancer Res*. 2012;10:1403-1418.
- Satoyoshi R, Kuriyama S, Aiba N, Yashiro M, Tanaka M. Asporin activates coordinated invasion of scirrhous gastric cancer and cancer-associated fibroblasts. *Oncogene*. 2015;34:650-660.
- Duval E, Bigot N, Hervieu M, et al. Asporin expression is highly regulated in human chondrocytes. *J Mol Med*. 2011;17:816-823.
- Nakajima M, Kizawa H, Saitoh M, Kou I, Miyazono K, Ikegawa S. Mechanisms for asporin function and regulation in articular cartilage. *J Biol Chem*. 2007;282:32185-32192.
- Gruber HE, Ingram JA, Hoelscher GL, Zinchenko N, Hanley EN, Sun Y. Asporin, a susceptibility gene in osteoarthritis, is expressed at higher levels in the more degenerate human intervertebral disc. *Arthritis Res Ther*. 2009;11:R47.
- Yamada S, Tomoeda M, Ozawa Y, et al. PLAP-1/Asporin, a novel negative regulator of periodontal ligament mineralization. *J Biol Chem*. 2007;282(32):23070-23080.
- Kizawa H, Kou I, Iida A, et al. An aspartic acid repeat polymorphism in asporin inhibits chondrogenesis and increases susceptibility to osteoarthritis. *Nat Genet*. 2005;37(2):138-144.
- Wang L, Wu H, Wang L, et al. Asporin promotes pancreatic cancer cell invasion and migration by regulating the epithelial to-mesenchymal transition (EMT) through both autocrine and paracrine mechanisms. *Cancer Lett*. 2017;398:24-36.
- Li H, Zhang Z, Chen L, et al. Cytoplasmic Asporin promotes cell migration by regulating TGF-beta/Smad2/3 pathway and indicates a poor prognosis in colorectal cancer. *Cell Death Dis*. 2019;10:109.
- Huo WU, Jing X, Cheng X, et al. Asporin enhances colorectal cancer metastasis through activating the EGFR/src/cortactin signaling pathway. *Oncotarget*. 2016;7:73402-73413.
- Ding Q, Zhang M, Liu C. Asporin participates in gastric cancer cell growth and migration by influencing EGF receptor signaling. *Oncol Rep*. 2015;33:1783-1790.
- Rochette A, Boufaied N, Scarlata E, et al. Asporin is a stromally expressed marker associated with prostate cancer progression. *Br J Cancer*. 2017;116:775.
- Zhan S, Li J, Ge W. Multifaceted roles of Asporin in cancer: current understanding. *Front Oncol*. 2019;9:948.
- Hurley PJ, Sundi D, Shinder B, et al. Germline variants in Asporin vary by race, modulate the tumor microenvironment, and are differentially associated with metastatic prostate cancer. *Clin Cancer Res*. 2016;22:448-458.
- Castellana B, Escuin D, Peiro G, et al. ASPN and GJB2 are implicated in the mechanisms of invasion of ductal breast carcinomas. *J Cancer*. 2012;3:175-183.
- Simkova D, Kharaisvili G, Korinkova G, et al. The dual role of asporin in breast cancer progression. *Oncotarget*. 2016;7:52045-52060.
- Maris P, Blomme A, Palacios AP, et al. Asporin is a fibroblast-derived TGF- $\beta$ 1 inhibitor and a tumor suppressor associated with good prognosis in breast cancer. *PLoS Medicine*. 2015;12:e1001871.
- Wu H, Jing X, Cheng X, et al. Asporin enhances colorectal cancer metastasis through activating the EGFR/Src/cortactin signaling pathway. *Oncotarget*. 2016;7(45):73402-73413.
- Zhang Z, Li H, Zhao Y, et al. Asporin promotes cell proliferation via interacting with PSMD2 in gastric cancer. *Front Biosci*. 2019;24:1178-1189.
- Fuyuhiko Y, Yashiro M, Noda S, et al. Upregulation of cancer-associated myofibroblasts by TGF- $\beta$  from scirrhous gastric carcinoma cells. *Br J Cancer*. 2011;105:996-1001.
- Yanagihara K, Kamada N, Tsumuraya M, Amano F. Establishment and characterization of a human gastric scirrhous carcinoma cell line in serum-free chemically defined medium. *Int J Cancer*. 1993;54:200-207.
- Yanagihara K, Takigahira M, Tanaka H, et al. Development and biological analysis of peritoneal metastasis mouse models for human scirrhous stomach cancer. *Cancer Sci*. 2005;96:323-332.
- Awata T, Yamada S, Tsushima K, et al. PLAP-1/Asporin positively regulates FGF-2 activity. *J Dental Res*. 2015;94:1417-1424.
- Hagiwara M, Ichiyanagi N, Kimura KB, Murakami Y, Ito A. Expression of a soluble isoform of cell adhesion molecule 1 in the brain and its involvement in directional neurite outgrowth. *Am J Pathol*. 2009;174:2278-2289.
- Kim S, Han J, Lee SK, et al. Berberine suppresses the TPA-induced MMP-1 and MMP-9 expressions through the inhibition of PKC- $\alpha$  in breast cancer cells. *J Surg Res*. 2012;176:e21-e29.

28. Wu W. The signaling mechanism of ROS in tumor progression. *Cancer Metastasis Rev.* 2006;25:695-705.
29. Kim JW, Tchernyshyov I, Semenza GL, Dang CV. HIF-1-mediated expression of pyruvate dehydrogenase kinase: a metabolic switch required for cellular adaptation to hypoxia. *Cell Metab.* 2006;3(3):177-185.
30. Tello D, Balsa E, Acosta-Iborra B, et al. Induction of the mitochondrial NDUFA4L2 protein by HIF-1 $\alpha$  decreases oxygen consumption by inhibiting Complex I activity. *Cell Metab.* 2011;14(6):768-779.
31. Semenza GL. Regulation of cancer cell metabolism by Hypoxia-inducible factor 1. *Semin Cancer Biol.* 2019;19:12-16.
32. Zhao T, Zhu Y, Morinibu A, et al. HIF-1-mediated metabolic reprogramming reduces ROS levels and facilitates the metastatic colonization of cancers in lungs. *Sci Rep.* 2014;4:3793.
33. Denko NC. Hypoxia, HIF1 and glucose metabolism in the solid tumor. *Nat Rev Cancer.* 2008;8(9):705-713.
34. Rius J, Guma M, Schachtrup C, et al. NF-kappaB links innate immunity to the hypoxic response through transcriptional regulation of HIF-1alpha. *Nature.* 2008;453(7196):807-811.
35. Hughes R, Simons BW, Khan H, et al. Asporin restricts mesenchymal stromal cell differentiation, alters the tumor microenvironment, and drives metastatic progression. *Cancer Res.* 2019;79:3636-3650.
36. Ludwig N, Szczepanski M, Gluszko A, et al. CD44(+) tumor cells promote early angiogenesis in head and neck squamous cell carcinoma. *Cancer Lett.* 2019;467:85-95.
37. Shida M, Kitajima Y, Nakamura J, et al. Impaired mitophagy activates mtROS/HIF-1 $\alpha$  interplay and increases cancer aggressiveness in gastric cancer cells under hypoxia. *Int J Oncol.* 2016;48:1379-1390.
38. Movafagh S, Crook S, Vo K. Regulation of hypoxia-inducible factor-1a by reactive oxygen species: New developments in an old debate. *J Cell Biochem.* 2015;116(5):696-703.
39. Wang S, Liu C, Yan P, et al. IL-1 beta increases asporin expression via the NF-kappaB p65 pathway in nucleus pulposus cells during intervertebral disc generation. *Sci Rep.* 2017;7(1):4112. <https://doi.org/10.1038/s41598-017-04384-3>

#### SUPPORTING INFORMATION

Additional supporting information may be found online in the Supporting Information section.

**How to cite this article:** Sasaki Y, Takagane K, Konno T, et al. Expression of asporin reprograms cancer cells to acquire resistance to oxidative stress. *Cancer Sci.* 2021;112:1251-1261. <https://doi.org/10.1111/cas.14794>